Interaction of SO_2 with CeO_2 and Cu/CeO_2 catalysts: photoemission, XANES and TPD studies

José A. Rodriguez[a,*], Tomas Jirsak[a], Andrea Freitag[a], Jonathan C. Hanson[a], John Z. Larese[a] and Sanjay Chaturvedi[b]

[a] *Department of Chemistry, Brookhaven National Laboratory, Upton, NY 11973, USA*
E-mail: rodrigez@bnl.gov
[b] *Analytical Research, Rohm and Haas Company, Spring House, PA 19477, USA*

Received 2 June 1999; accepted 18 August 1999

CeO_2 and Cu/CeO_2 are effective catalysts/sorbents for the removal or destruction of SO_2. Synchrotron-based high-resolution photoemission, X-ray absorption near-edge spectroscopy (XANES), and temperature-programmed desorption (TPD) have been employed to study the reaction of SO_2 with pure and reduced CeO_2 powders, ceria films (CeO_2, CeO_{2-x}, Ce_2O_{3+x}) and model Cu/CeO_2 catalysts. The results of XANES and photoemission provide evidence that SO_4 was formed upon the adsorption of SO_2 on pure powders or films of CeO_2 at 300 K. The sulfate decomposed in the 390–670 K temperature range with mainly SO_2 and some SO_3 evolving into gas phase. At 670 K, there was still a significant amount of SO_4 present on the CeO_2 substrates. The introduction of O vacancies in the CeO_2 powders or films favored the formation of SO_3 instead of SO_4. Ceria was able to fully dissociate SO_2 to atomic S only if Ce atoms with a low oxidation state were available in the system. When Cu atoms were added to CeO_2 new active sites for the destruction of SO_2 were created improving the catalytic activity of the system. The surface chemistry of SO_2 on the Cu-promoted CeO_2 was much richer than on pure CeO_2. The behavior of ceria in several catalytic processes (oxidation of SO_2 by O_2, reduction of SO_2 by CO, automobile exhaust converters) is discussed in light of these results.

Keywords: cerium oxides, SO_2, desulfurization, copper, X-ray absorption spectroscopy, photoemission and XPS

1. Introduction

In the area of environmental catalysis a lot of attention is focused on the development of catalysts that have a high activity for the destruction or conversion of sulfur dioxide (DeSOx process) [1–3]. Sulfur dioxide is one of the major pollutants released to the atmosphere as a result of volcanic activity and the combustion of fuels in power plants, factories, houses and transportation [4]. After oxidation and reaction with water in the atmosphere, it is responsible for acid rain that kills vegetation and leads to the corrosion of buildings and monuments [4]. Furthermore, the SO_2 produced by combustion of sulfur-containing impurities present in all gasolines deactivates catalytic converters employed for the control CO and NO_x emissions from automobile engines [5]. Thus, there is a clear need to minimize the negative effects of SO_2 in our industrial society.

A detailed study of the interaction of SO_2 with CeO_2 and Cu/CeO_2 is interesting for several reasons. First, catalysts containing ceria are effective for the oxidation of SO_2 and adsorption of the resulting product as a sulfate [6,7]:

$$SO_2(\text{gas}) + nO_2(\text{gas}) \rightarrow SO_x(\text{ads}) \qquad (1)$$

Second, CeO_2 doped with copper or other metals is able to catalyze the reduction of SO_2 by CO [8]:

$$2CO(\text{gas}) + SO_2(\text{gas}) \rightarrow 2CO_2(\text{gas}) + S(\text{ads}) \qquad (2)$$

And third, adsorption of SO_2 affects the performance of ceria in automotive catalytic converters [5,6]. In these systems, CeO_2 releases oxygen and thereby assists the oxidation of hydrocarbons and CO under fuel-rich conditions [6]. This property results from the fact that cerium is stable in 3+ and 4+ oxidation states, which allows the oxide to shift between CeO_2 and CeO_{2-x} depending on the fuel/O_2 ratio [6].

In this letter, we use the high-resolution of synchrotron-based photoemission and X-ray absorption near-edge spectroscopy (XANES) to study the interaction of SO_2 with ceria powders plus model CeO_x and Cu/CeO_x catalysts. The effects of temperature, Ce oxidation state, and Cu promotion are investigated. The measurements at the S K-edge in XANES allow us a precise identification of the formation of SO_3 and SO_4 species in the oxide systems.

2. Experimental

2.1. Work with ceria films

The experiments described in section 3 for polycrystalline films of ceria were carried out in an ultrahigh-vacuum (UHV) chamber that is part of the U7A beamline of the National Synchrotron Light Source (NSLS) at Brookhaven National Laboratory [9]. The UHV chamber is equipped with optics for low-energy electron diffraction (LEED), a hemispherical electron energy analyzer with multichannel detection for photoelectron spectroscopy,

---

[*] To whom correspondence should be addressed.

a Mg Kα X-ray source, and a quadrupole mass spectrometer. Films of CeO_2 were deposited on a Pt(111) crystal by evaporating Ce metal (Johnson Mathey, 99.9%) onto the substrate held at 450 K in the presence of 1×10^{-6} Torr of O_2 [10]. Following ceria deposition, the samples were oxidized in 1×10^{-5} Torr of O_2 for 20 min at 450 K to ensure complete oxidation of the cerium metal. The oxide films were polycrystalline (LEED results) and exhibited the typical Ce 3d, O 1s and valence spectra of bulk CeO_2 [11–13]. From the attenuation of the peaks for the Pt substrate in photoemission [14], we estimate a thickness of 30–40 Å for the CeO_2 films. By working with these ultra-thin films, we prevented effects of charging in the photoemission experiments with the synchrotron beam. This is a big advantage when dealing with semiconductors or insulators [11,14].

Metallic Cu (Johnson Mathey, 99.999%) was vapor-deposited on CeO_2 surfaces at 300 K. The atomic flux from the Cu doser was calibrated following the same methodology employed in a previous work for the Cu/Pt(111) system [15]. High-purity sulfur dioxide (Mattheson) was dosed to the ceria and copper/ceria systems either from the background by backfilling the main UHV chamber (small doses) or by moving the samples to an attached reaction cell (1–1.5 Torr doses). For the small doses, the coverage of sulfur species on the surfaces was determined by measuring the area under the S 2p features, which was scaled to absolute values by comparing it to the corresponding area for 0.33 monolayers (ML) of S on Pt(111) [16]. In this work, the coverages of S and Cu on ceria are reported with respect to the number of Pt(111) atoms, i.e., 1.51×10^{15} adatoms cm^{-2} corresponds to $\theta = 1$ ML.

2.2. Work with ceria powders

The experiments with powders of CeO_2 (Alfa-Aesar, 99.99%) were performed in a RXM-100 instrument from Advanced Scientific Designs. Before exposure to SO_2, the CeO_2 powders were heated in vacuum at 673 K for 10 min to induce the removal of OH groups that could be present on the surface [8]. The powders were then exposed to 500 Torr of a 30% O_2 + 70% He mixture at 400 K for 15 min to remove oxygen vacancies. Characterization with X-ray photoelectron spectroscopy (XPS) and XANES showed systems that had the typical Ce 3d, O 1s and O K-edge spectra of CeO_2 [11,12]. Partial reduction of the oxide powders was carried out in a flow reactor with a gas mixture of 15% H_2 + 85% He (total flow rate 80 cm^3/min) at temperatures of 473 and 773 K, with subsequent exposure to atmospheric oxygen. The dosing of SO_2 to the pure and reduced CeO_2 samples was done in a batch reactor at 323 K under a constant SO_2 pressure of 10 Torr for 10 min. After the dosing of SO_2, temperature-programmed desorption (TPD) spectra were taken with a heating rate of 20 K/min and He as the carrier gas (80 cm^3/min). The chemical analysis of the desorbing products was performed employing a quadrupole mass spectrometer. The X-ray powder diffraction patterns of the reduced and sulfided ceria were recorded at beamline X7B of the NSLS using a MAR-345 detector. The S K-edge spectra in XANES were obtained at beamline X19-A in the "fluorescence yield mode" with a Stern–Heald–Lytle detector. Beamline U7A was employed to take the O K-edge XANES spectra, which were collected in the "electron yield mode" using a channeltron multiplier near the sample surface. The XPS data were taken in a KRATOS-ULTRA ESCA instrument using a monochromatized Al Kα source and an electron gun for charge compensation.

3. Results

3.1. Interaction of SO_2 with CeO_2 and CeO_x

Figure 1 compares S 2p photoemission results for the adsorption of 5 L (1 L = 1 langmuir = 10^{-6} Torr s) of sulfur dioxide on metallic cerium, and several ceria films. Different sulfur species are observed on the surfaces depending on the oxidation state of the cerium atoms. The CeO_2 system was prepared as described in section 2.1. It showed the characteristic Ce 3d, O 1s and valence features of bulk CeO_2 [11–13]. In its valence photoemission spectrum (figure 2) there was no signal in the region between 0 and 3 eV where Ce^{3+} appears [11]. The CeO_{2-x} system was prepared by sputtering a CeO_2 film with Ar^+

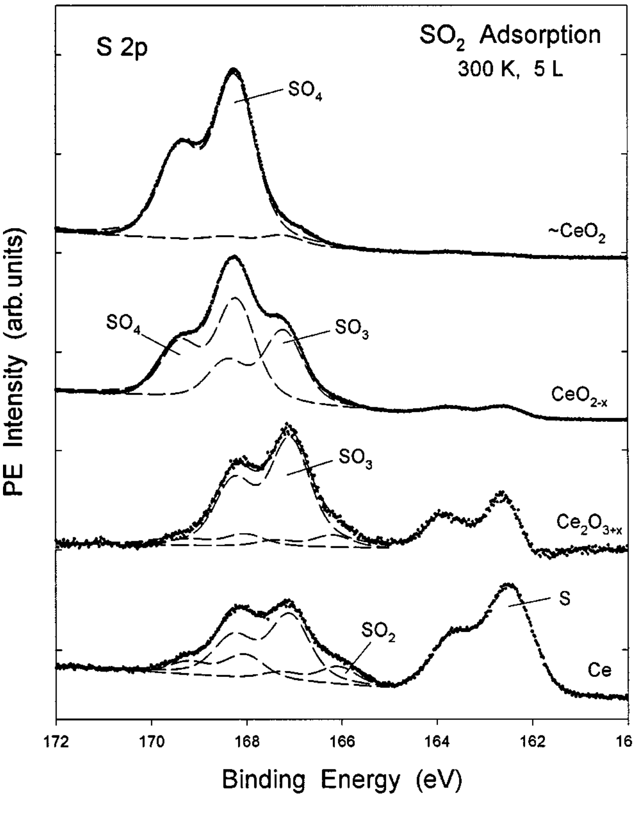

Figure 1. S 2p photoemission spectra acquired after dosing 5 L of sulfur dioxide to Ce, Ce_2O_{3+x}, CeO_{2-x}, and CeO_2 polycrystalline films at 300 K. The spectra were curve-fitted following the procedure described in [18,19]. The electrons were excited using a photon energy of 260 eV.

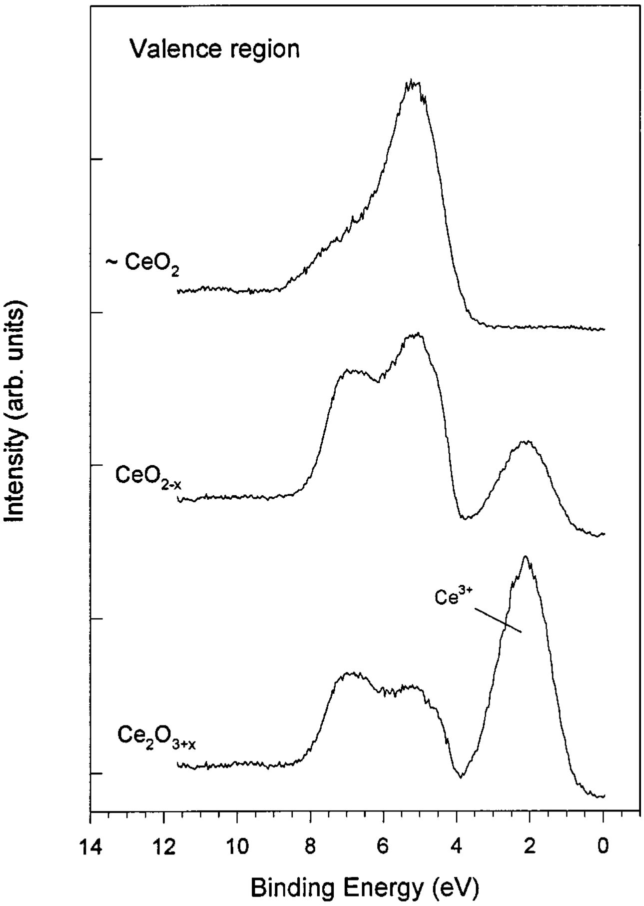

Figure 2. Valence photoemission spectra acquired before dosing SO_2 to the Ce_2O_{3+x}, CeO_{2-x}, and CeO_2 systems in figure 1. A photon energy of 325 eV [11] was used to take these spectra.

ions [11,13]. This preferentially removed O atoms [11,13] and led to the appearance of peaks for Ce^{3+} in the Ce 3d and valence (figure 2) spectra. To prepare the Ce_2O_{3+x} system, a film of metallic Ce was exposed to a limited amount of O_2 at room temperature and then annealed to 600 K [11,17]. The Ce 3d and valence (figure 2) photoemission data for this system showed mainly the typical features for Ce^{3+} [11] and some Ce^{4+}. Thus, on the basis of photoemission results [11,13,17], one can see clear differences for the oxidation state of cerium in the systems of figure 1: from 0 in metallic Ce to mainly 3+ (Ce_2O_{3+x}) or 4+ (CeO_{2-x}), and, finally, to only 4+ in CeO_2.

For the adsorption of SO_2 on cerium metal, the S 2p spectra showed two different types of features: atomic sulfur between 162 and 164 eV and SO_x species between 166 and 169 eV (see figure 1). At small exposures of SO_2 (<1 L) only features for atomic sulfur were seen, indicating the full decomposition of the molecule ($SO_2 \rightarrow S(ads) + 2O(ads)$). As the coverages of atomic S and O increased on the surface, adsorbed SO_x species became stable and a complex structure appeared in the S 2p region from 166 to 169 eV. In general, this structure could be curve-fitted [18,19] by a set of three doublets (see figure 1), with the most intense $2p_{3/2}$ peak appearing around

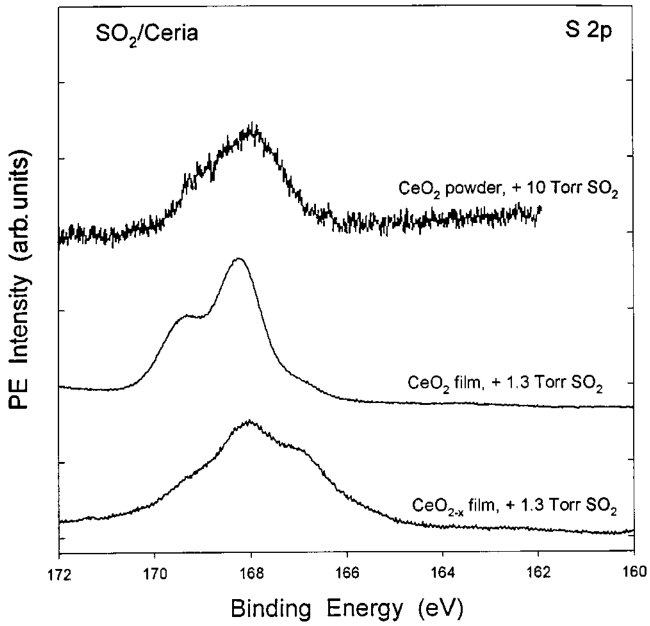

Figure 3. S 2p spectra for the adsorption of SO_2 on a CeO_2 powder and ceria films at 300 K. The XPS spectrum in the top was taken using monochromatized Al Kα radiation. A synchrotron beam with a photon energy of 260 eV was employed to collect the spectra in the middle and bottom of the figure.

167 eV. This binding energy is too high to be assigned to adsorbed SO_2 [19]. Also, it corresponds to a separation of 4–4.5 eV with respect to atomic sulfur which is substantially smaller than the separation 5–6 eV observed for SO_4 groups[1] [20,21]. Thus, we tentatively assign the species at a binding energy of 167 eV to SO_3. This is the dominant species after dosing SO_2 to the Ce_2O_{3+x} system. The species is also present on CeO_{2-x}, but now the most intense S 2p features appear between 168 and 170 eV and correspond to SO_4 [20,21]. Upon dosing of SO_2 to the CeO_2 film essentially only SO_4 is formed. From the trends in figure 1 one can reach two important conclusions. First, as the average oxidation state of Ce increases, the ability of the system to dissociate S–O bonds clearly diminishes. Second, the introduction of O vacancies in the CeO_2 system favors the formation of SO_3 at the expense of SO_4.

In figure 1 the doses of SO_2 were small and the total sulfur coverages (S + SO_x) were estimated to be in the range of 0.5–0.7 ML. Total sulfur coverages much larger than 1 ML were found after exposing the CeO_2 and CeO_{2-x} films to 1.3 Torr of SO_2 at 300 K during 5 min in a reaction cell attached to the UHV chamber. The resulting S 2p spectra are displayed in figure 3. Again, one finds that SO_4 is the predominant species on CeO_2, with a mixture of SO_4 and SO_3 on CeO_{2-x}. The photoemission spectrum for the CeO_2 film is similar to a S 2p XPS spectrum obtained after

---

[1] In [20], a difference of 5–5.7 eV is observed between the S 2p binding energies of S and SO_4 on alumina. A separation of ~5 eV is reported in [21] for the S $2p_{3/2}$ binding energies of S and SO_4 on Pt(111), whereas a difference of 3–3.5 eV is observed between the S $2p_{3/2}$ binding energies of chemisorbed S and SO_2.

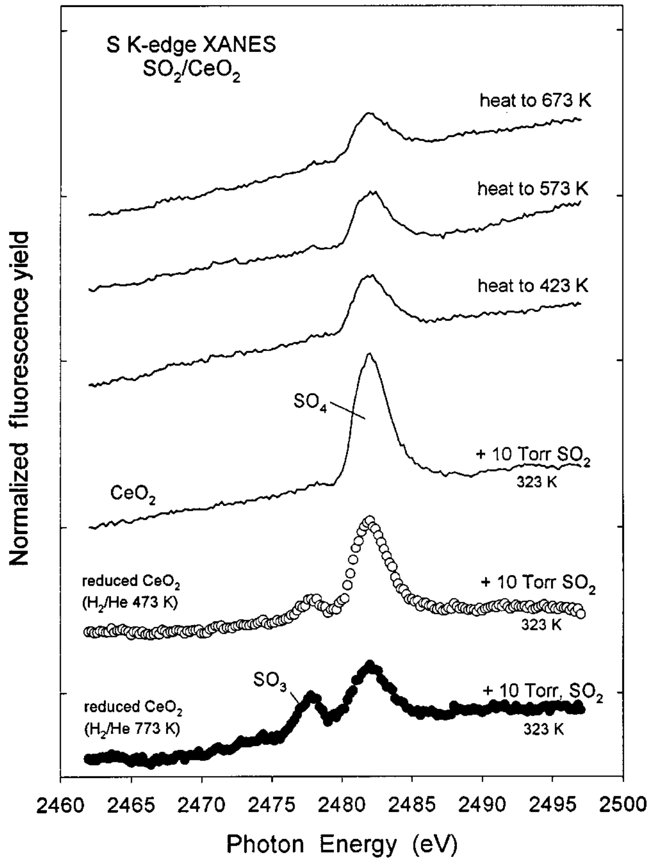

Figure 4. S K-edge XANES data for the adsorption of SO_2 on pure (solid traces) and partially reduced (dotted traces) powders of CeO_2. The CeO_2 and CeO_{2-x} systems were exposed to SO_2 at 323 K. The SO_2/CeO_2 sample was heated to 423, 573, and 673 K under vacuum. All the spectra were acquired at room temperature.

exposing a powder of bulk CeO_2 to 10 Torr of SO_2 for 10 min at 323 K.

The interaction between SO_2 and CeO_2 powders was studied using XANES. The results of measurements at the S K-edge are shown at the top of figure 4 (solid traces). For the SO_2/CeO_2 system at 323 K, the data show a single peak at a photon energy of 2481.6 eV. In the past, we have found that the position of the S K-edge for adsorbed sulfur species is very sensitive to the oxidation state of sulfur [22,23]. When the value of 2481.6 eV is compared with typical standards [22,23] (figure 5), one finds a clear and definitive proof that SO_4 can be formed by reaction of SO_2 with pure CeO_2. This is corroborated by the O K-edge data in figure 6. The O K-edge for pure CeO_2 exhibits three peaks that have been assigned to electronic transitions from the O 1s core levels into the empty cerium 4f, $5de_g$ and $5dt_g$ levels [11]. After exposing the CeO_2 powder to SO_2, one sees an increase in the intensity of the features around a photon energy of 538 eV where the main peak for sulfate compounds [22] ($Ce_2(SO_4)_3$, for example) appears in the O K-edge.

In figures 4 and 6, there is a decrease in the intensity for the SO_4 signal of SO_2/CeO_2 upon heating of the sample to elevated temperatures, but at 673 K there is still

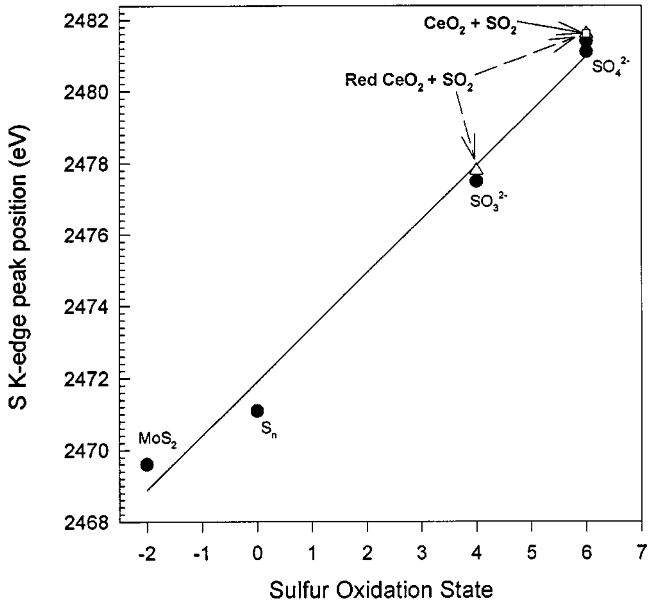

Figure 5. S K-edge XANES peak positions for SO_x species on pure (□, solid arrow) and reduced CeO_2 (△, dashed arrow), plus a series of standards (MoS_2, S_n, Na_2SO_3, Na_2SO_4, and $Ce_2(SO_4)_3$ (●)) [22,23]. The values for the reference compounds are fitted to a straight line.

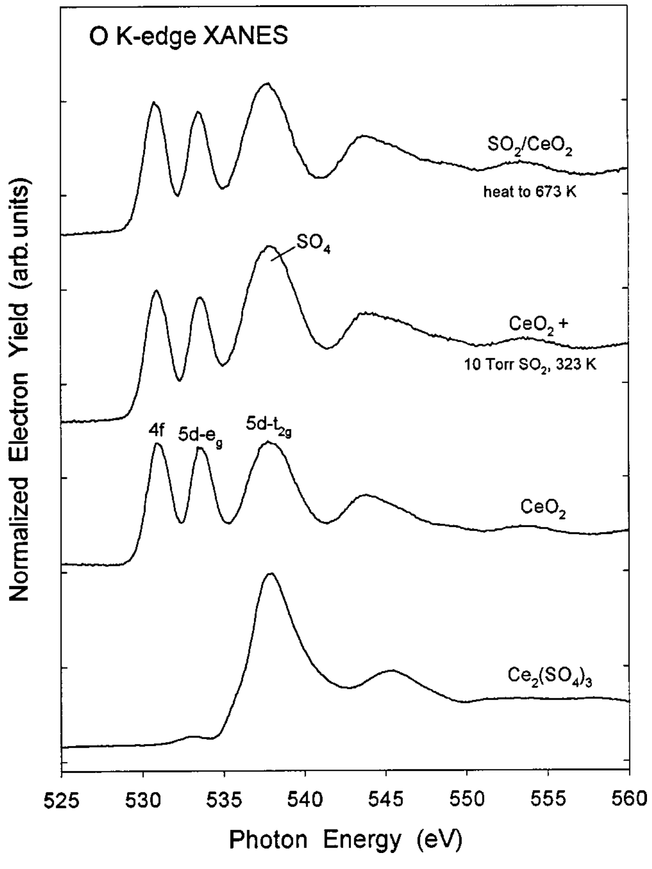

Figure 6. O K-edge XANES spectra for powders of $Ce_2(SO_4)_3$, pure CeO_2, CeO_2 exposed to SO_2 at 323 K, and the SO_2/CeO_2 sample heated to 673 K in vacuum. All the spectra were recorded at room temperature.

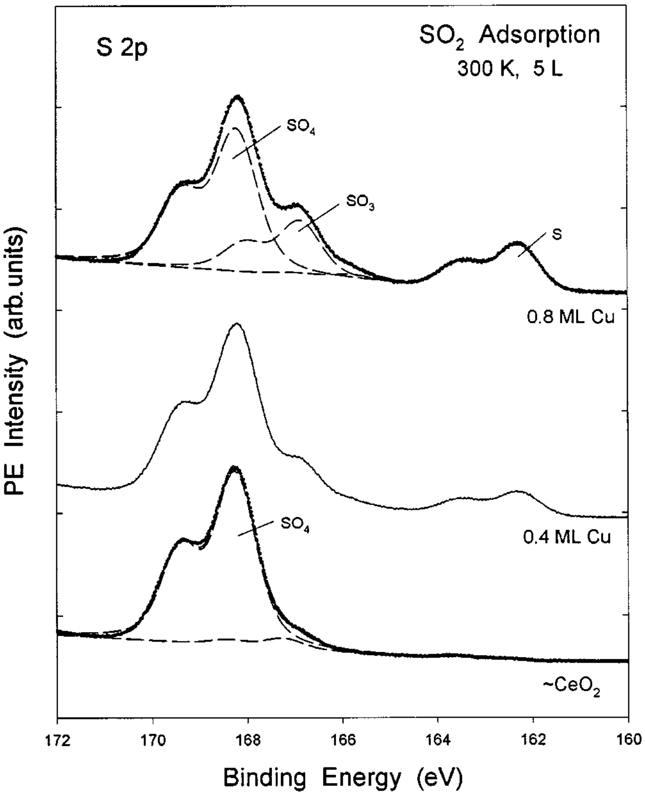

Figure 7. S 2p photoemission spectra acquired after dosing 5 L of sulfur dioxide to pure CeO_2 and Cu/CeO_2 systems with copper coverages of 0.4 and 0.8 ML. The spectra were curve-fitted following the procedure described in [18,19]. The electrons were excited using a photon energy of 260 eV.

a significant amount of sulfate present in the system. In previous TPD studies for SO_2/ceria [24], desorption of molecular SO_2 was observed between 350 and 700 K with a maximum at ~400 K. We found similar TPD results after heating our SO_2/CeO_2 powders, but in addition there was a weak yet clear signal for desorption of SO_3 in the 390–700 K temperature range. No signal for desorption of SO_4 was seen. Thus, in the SO_2/CeO_2 system, the sulfate decomposes with mainly SO_2 evolving into gas phase and a substantial fraction of the oxygen remaining bonded in a matrix of cerium oxide.

In a separate set of experiments, we investigated the interaction of SO_2 with partially reduced CeO_2 powders. Samples of pure CeO_2 were first exposed to a stream of H_2(15%)/He(85%) in a flow reactor at 473 and 773 K, and then to atmospheric oxygen at room temperature. This produced compounds that had the same X-ray powder diffraction pattern of CeO_2 with only minor extra broadening in the lines. Their Ce 3d XPS spectra showed a small amount of Ce^{3+} [11,12], and their O K-edge structure in XANES was much closer to CeO_2 than to Ce_2O_3 [11]. Based on this, the reduced powders can be classified as CeO_{2-x}. The bottom part of figure 4 shows S K-edge XANES data for the adsorption of SO_2 on the reduced CeO_2 samples (dotted traces). In these systems two peaks with photon energies of 2477.8 and 2481.8 eV are clearly seen. They indicate the presence of SO_3 and SO_4 species on the oxide surfaces (see figure 5). The introduction of O vacancies in bulk CeO_2 favors the formation of SO_3 instead of SO_4, as was found in the case of the ceria films in figure 1.

3.2. Interaction of SO_2 with Cu/CeO_2

Copper-doped CeO_2 is used as a catalyst for the reduction of SO_2 by CO [8]. Figure 7 compares S 2p photoemission results for the adsorption of SO_2 on clean and Cu-promoted CeO_2 films ($\theta_{Cu} = 0.4$ and 0.8 ML). In these experiments, copper atoms were vapor-deposited on CeO_2 films at 300 K and the resulting Cu/CeO_2 systems were exposed to 5 L of SO_2. The chemistry of sulfur dioxide on the copper-promoted surfaces is much richer than on pure CeO_2. After curve-fitting [18,19] the S 2p spectra for the $SO_2/Cu/CeO_2$ systems, one sees clear features for SO_4, SO_3 and S. Perhaps the most important result is that copper facilitates the full decomposition of SO_2 and a significant amount of atomic sulfur is deposited on the surface.

4. Discussion

The results of XANES and photoemission provide evidence that SO_4 can be formed upon the adsorption of sulfur dioxide on pure CeO_2. The formation of SO_4 could take place through a reaction like

$$CeO_2(\text{solid}) + 4SO_2(\text{gas}) \rightarrow 2SO(\text{gas}) + Ce(SO_4)_2(\text{solid}) \qquad (3)$$

which is exothermic ($\Delta H = -14$ kcal/mol [25]).[2] In studies for the adsorption of SO_2 on metals [19,26], it has been found that SO_2 can undergo disproportionation producing SO_4/SO_3 species on the surface and gaseous SO. In addition, due to the high stability of cerium sulfates [25], SO_4 groups also can be formed on CeO_2 as a result of reactions that do not involve the production of SO [1,19,24,26]. Our results show that the introduction of O vacancies in the CeO_2 system favors the formation of SO_3 at the expense of SO_4. Recent studies for the adsorption of SO_2 on defective single-crystal faces of CeO_2 show the presence of SO_x groups that can be assigned to SO_4/SO_3 surface species [27]. In an early work [24] that dealt with the interaction of SO_2 and ceria powders, the formation of adsorbed SO_3 at room temperature was proposed on the basis of IR results. The SO_3 was not stable and transformed into SO_4 at higher temperatures [24]. Heating of ceria in the presence of SO_2 gas at 373 K led to the production of SO_4 species in the bulk and surface of the samples [24b]. These trends are consistent with the results in figure 4 which indicate that SO_4 can be very stable on CeO_2.

CeO_2 supported on alumina and a $Mg_2Al_2O_5$ spinel is a good catalyst for the destruction of the SO_2 produced by

---

[2] The enthalpy change for reaction (3) was calculated using the heats of formation [25] of CeO_2 (−260.2 kcal/mol), $Ce(SO_4)_2$ (−560 kcal/mol), SO_2 (−70.9 kcal/mol), and SO (1.2 kcal/mol).

the burning of coke during the cleaning of fluid-catalytic cracking (FCC) units in oil refineries [7]. This process involves three steps:

$$2SO_2 + O_2 \rightarrow 2SO_3 \qquad (4)$$

$$SO_3 + \text{MetalO} \rightarrow \text{MetalSO}_4 \qquad (5)$$

$$\text{MetalSO}_4 + 4H_2 \rightarrow \text{MetalO} + H_2S + 3H_2O \qquad (6)$$

In the first, CeO_2 catalyzes the oxidation of SO_2 by O_2. Once SO_3 is formed, it has to be adsorbed by the catalyst. In this second step, it has been postulated that the alumina or $Mg_2Al_2O_5$ support acts as the "sink" for the produced SO_3 [7]. Our results indicate that ceria has a strong chemical affinity for SO_x species and must also play an active role in the trapping of the SO_3. In the final step, the catalyst is regenerated with H_2 and sulfur evolves as H_2S into gas phase. To be effective this regeneration has to occur at very high temperatures due to the large thermal stability of SO_4 on CeO_2, as illustrated in figure 4.

Ceria promoted/doped with copper is an active catalyst for the reduction of SO_2 by CO [8]:

$$2CO(\text{gas}) + SO_2(\text{gas}) \rightarrow 2CO_2(\text{gas}) + S(\text{ads}) \qquad (2)$$

In this process the SO_2 is completely decomposed and oxygen is removed from the system by formation of CO_2. The results in figure 1 indicate that ceria is able to dissociate SO_2 only when Ce atoms with a low oxidation state are available. This is due to the fact that the metal needs to donate electrons into the LUMO of SO_2 (S–O antibonding orbital) in order to be able to dissociate the molecule [19]. Since Ce is relatively easy to oxidize at low temperatures,[3] reaction (2) can be efficient only at high temperatures (which facilitate the removal of oxygen from the system [8]) and with a CO/SO_2 ratio in the feed $\geqslant 2$. When Cu atoms are added to CeO_2 new active sites for the destruction of SO_2 are created (see figure 7) and, indeed, the performance of the catalyst substantially improves [8]. From a practical viewpoint, the use of copper introduces two big advantages. First, copper does not exhibit a tendency to adopt high oxidation states as cerium does [28]. Second, it is much easier to reduce copper oxides with CO [29] than to reduce ceria [8]. Thus, Cu sites eventually will remain catalytically active for a longer period of time than Ce sites.

The SO_2 yielded by the combustion of sulfur-containing impurities present in the gasoline affects the activity of automotive catalytic converters that contain CeO_2 and metals like Pd and Rh [5,6]. The adsorption of SO_2 on surfaces of Pd and Rh at 300 K produces atomic S and SO_4/SO_3 species that decompose, $n\text{SO}_x(\text{ads}) \rightarrow \text{SO}_2(\text{gas}) + \text{S}(\text{ads}) + \text{O}(\text{ads})$, at temperatures below 450 K [30]. In contrast, the SO_4 groups are stable on ceria up to temperatures above 700 K. Thus, ceria may act as a scrubber of SO_2 preventing the poisoning of the metal catalysts by sulfur but, in the long term, the formed SO_4 will reduce the ability that ceria has to release oxygen and assist in the oxidation of hydrocarbons and CO under fuel-rich conditions.

5. Conclusions

The O centers in CeO_2 are very efficient for oxidizing and trapping SO_2. The results of XANES and photoemission provide evidence that SO_4 can be formed upon the adsorption of SO_2 on CeO_2 at 300 K. Part of the sulfate decomposes in the 390–670 K temperature range with SO_2 and some SO_3 evolving into gas phase. At 670 K, a substantial amount of SO_4 still remains on the CeO_2 substrate.

The introduction of O vacancies in CeO_2 favors the formation of SO_3 at the expense of SO_4. Ceria is able to fully dissociate SO_2 to atomic sulfur only if cerium atoms with a low oxidation state are available in the system. When Cu atoms are added to CeO_2 new active sites for the destruction of SO_2 are created improving the performance of the system as a catalyst for the reduction of SO_2 by CO.

Acknowledgement

This research was carried out at Brookhaven National Laboratory under contract DE-AC02-98CH10086 with the US Department of Energy (Divisions of Chemical Sciences and Materials Science) and made possible by Laboratory Directed Research and Development Funding (LDRD99-62). The NSLS is supported by the divisions of Materials and Chemical Sciences of the US Department of Energy.

References

[1] A. Pieplu, O. Saur and J.-C. Lavalley, Catal. Rev. Sci. Eng. 40 (1998) 409.
[2] J.A. Rodriguez and J. Hrbek, Acc. Chem. Res. (1999), in press.
[3] J.M. Thomas and W.J. Thomas, *Principles and Practices of Heterogeneous Catalysis* (VCH, New York, 1997).
[4] A.C. Stern, R.W. Boubel, D.B. Turner and D.L. Fox, *Fundamentals of Air Pollution*, 2nd Ed. (Academic Press, Orlando, 1984).
[5] K.C. Taylor, Catal. Rev. Sci. Eng. 35 (1993) 457.
[6] A. Trovarelli, Catal. Rev. Sci. Eng. 38 (1996) 439.
[7] A.A. Bhattacharyya, G.M. Woltermann, J.S. Yoo, J.A. Karch and W.E. Cormier, Ind. Eng. Chem. Res. 27 (1988) 1356.
[8] A. Tschope, W. Liu, M. Flytzani-Stephanopoulos and J.Y. Ying, J. Catal. 157 (1995) 42.
[9] J.A. Rodriguez, T. Jirsak and J. Hrbek, J. Phys. Chem. B 103 (1999) 1966.
[10] E.S. Putna, R.J. Gorte, J.M. Vohs and G.W. Graham, J. Catal. 178 (1998) 598.
[11] D.R. Mullins, S.H. Overbury and D.R. Huntley, Surf. Sci. 409 (1998) 307.
[12] J.Z. Shyu, W.H. Weber and H.S. Gandhi, J. Phys. Chem. 92 (1988) 4964.
[13] J. Stubenrauch and J.M. Vohs, J. Catal. 159 (1996) 50.
[14] D.W. Goodman, Chem. Rev. 95 (1995) 523.
[15] J.A. Rodriguez, C.M. Truong and D.W. Goodman, J. Chem. Phys. 96 (1992) 7814.
[16] J.A. Rodriguez, M. Kuhn and J. Hrbek, Chem. Phys. Lett. 251 (1996) 13.

---

[3] For example, at 300 K under a SO_2-rich environment, reactions like $Ce + 2SO_2 \rightarrow 2SO + CeO_2$ ($\Delta H = -116$ kcal/mol [25]) and (3) will lead to deactivation of the catalyst.

[17] C. Hardacre, G.M. Roe and R.M. Lambert, Surf. Sci. 326 (1995) 1.
[18] J. Hrbek, S.Y. Li, J.A. Rodriguez, D.G. van Campen, H. Huang and G.-Q. Xu, Chem. Phys. Lett. 267 (1997) 65.
[19] J.A. Rodriguez, T. Jirsak, S. Chaturvedi and J. Hrbek, J. Am. Chem. Soc. 120 (1998) 11149.
[20] K. Wilson, A.F. Lee, C. Hardacre and R.M. Lambert, J. Phys. Chem. 102 (1998) 1736.
[21] M. Polcik, L. Wilde, J. Haase, B. Brena, G. Comelli and G. Paolucci, Surf. Sci. 381 (1997) L568.
[22] S. Chaturvedi, J.A. Rodriguez and J.L. Brito, Catal. Lett. 51 (1998) 85.
[23] J.A. Rodriguez, S. Chaturvedi, J.C. Hanson and J.L. Brito, J. Phys. Chem. B 103 (1999) 770.
[24] (a) M. Waqif, A.M. Saad, M. Bensitel, J. Bachelier, O. Saur and J.-C. Lavalley, J. Chem. Soc. Faraday Trans. 88 (1992) 2931; (b) M. Waqif, P. Bazin, O. Saur, J.-C. Lavalley, G. Blanchard and O. Touret, Appl. Catal. B 11 (1997) 193.
[25] *Lange's Handbook of Chemistry*, 13th Ed. (McGraw-Hill, New York, 1985) table 9-1.
[26] S. Chaturvedi, J.A. Rodriguez, T. Jirsak and J. Hrbek, J. Phys. Chem. B 102 (1998) 7033.
[27] D. Mullins, private communication.
[28] J. Emsley, *The Elements* (Clarendon Press, Oxford, 1989) pp. 46, 54.
[29] C.T. Campbell, K.A. Daube and J.M. White, Surf. Sci. 182 (1987) 458.
[30] J.A. Rodriguez, T. Jirsak and S. Chaturvedi, J. Chem. Phys. 110 (1999) 3138.